

Electronic Supplementary Information

Energy Landscape of a Hydrogen-Bonded Nondegenerate Molecular Shuttle

D. Deniz Günbaş, Leszek Zalewski, Albert M. Brouwer*

*van 't Hoff Institute for Molecular Sciences, University of Amsterdam,
Nieuwe Achtergracht 129, 1018 WS Amsterdam, The Netherlands*

Email: A.M.Brouwer@uva.nl

Table of Contents

1. MATERIALS.....	3
2. GENERAL METHODS.....	3
3. SYNTHESIS OF ROTAXANES 1 AND 4 AND THE CORRESPONDING THREADS 3 AND 5	4
4. DETAILS OF SYNTHESIS AND CHARACTERIZATION	6
5. NMR SPECTRA.....	10
6. VARIABLE TEMPERATURE ¹H-NMR SPECTRA	14
7. POPULATIONS OF TRANSLATIONAL ISOMERS.....	17
8. REFERENCES	20

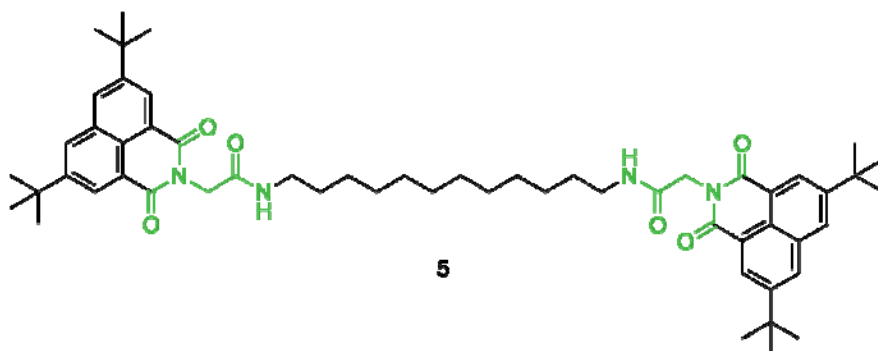
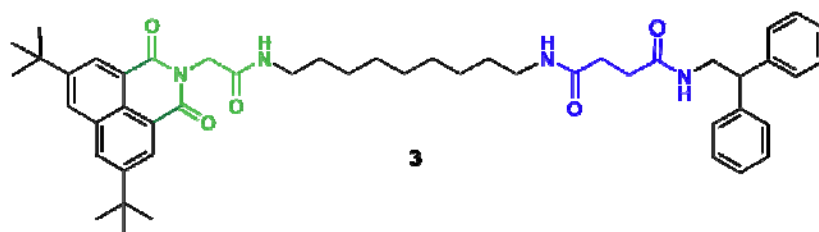
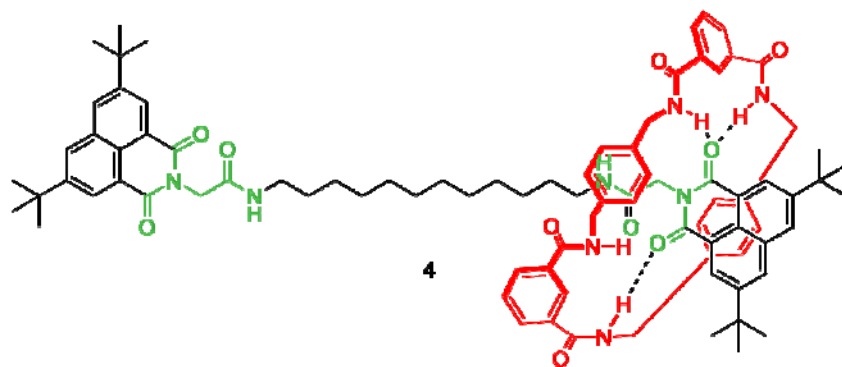
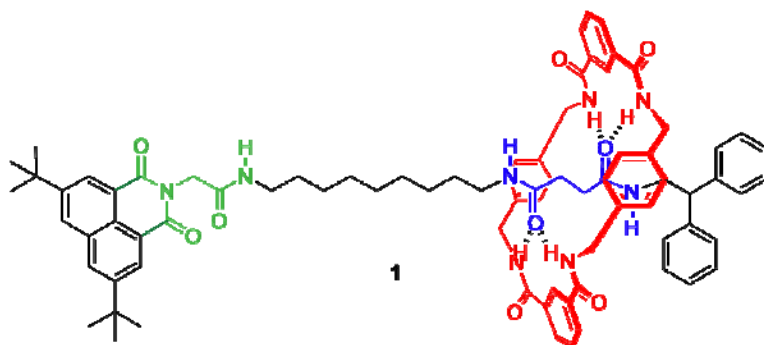
1. Materials

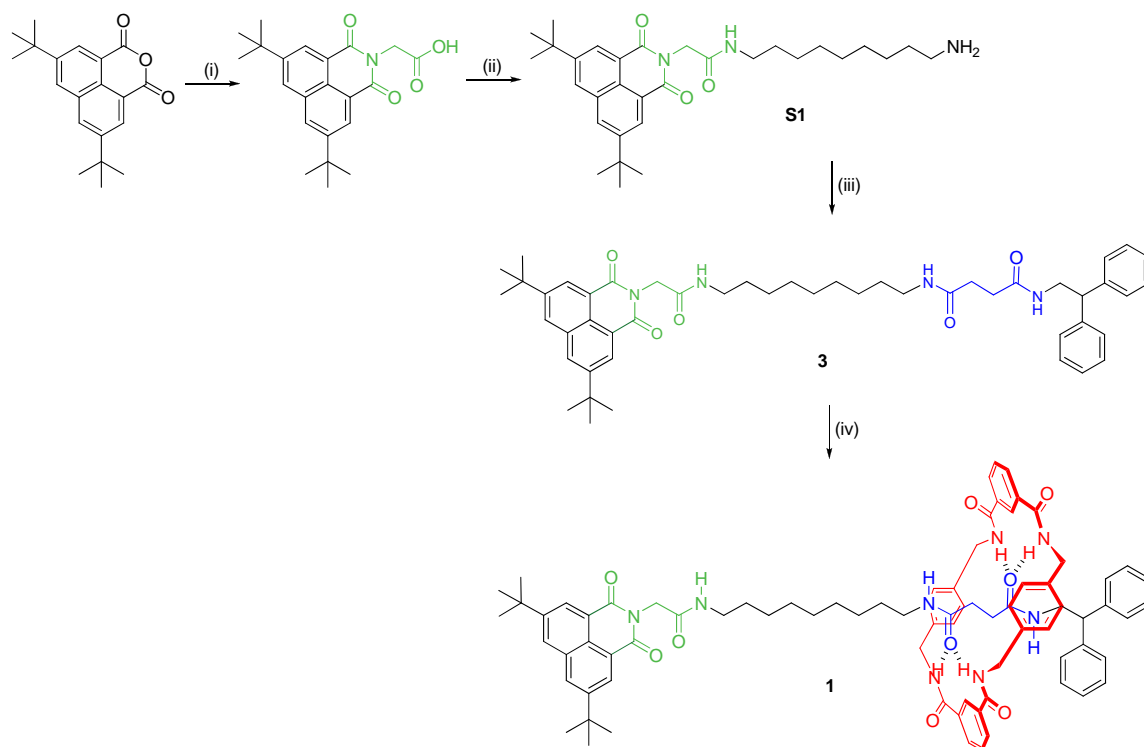
All reagents were purchased from Sigma Aldrich or Fluka, and used as received. All reactions were carried out under an inert nitrogen or argon atmosphere. THF was dried and deoxygenated by distillation over sodium benzophenone under an atmosphere of argon. MeOH was distilled from Mg prior to use. The following compounds were prepared according to literature procedures: *N*-(2,2-diphenylethyl)-succinamic acid,¹ 2,5-Di-*tert*-butylacenaphthylidic anhydride,² 2-(acetic acid)-5-8-di-*tert*-butyl-benzo[de]isoquinoline-1,3-dione³ and *N*-Boc-1,9-diaminododecane.⁴

2. General methods

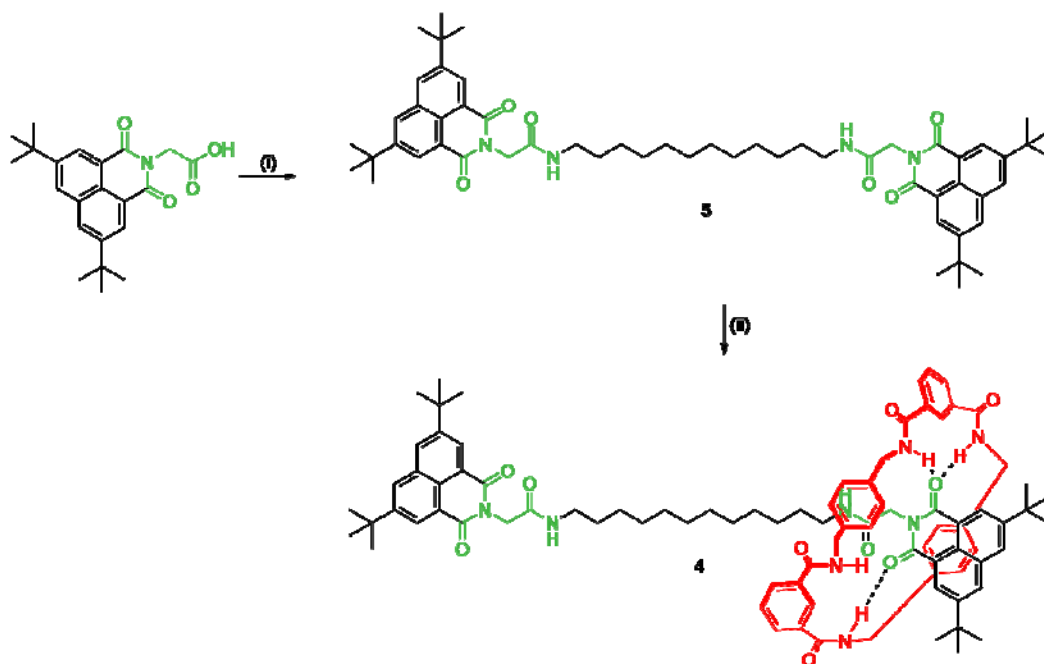
The 1D and 2D NMR spectra were recorded on a Bruker Avance 400 or Varian 500 spectrometers operating at 400 and 500 MHz, respectively, for ¹H NMR. Chemical shifts are in parts per million (ppm) using residual solvent peaks as internal references. Coupling constants (*J*) are reported in hertz (Hz). The full assignment of the ¹H NMR signals was performed using COSY (correlation spectroscopy) and NOESY (nuclear overhauser effect spectroscopy) experiments. Standard abbreviations indicating multiplicity were used as follows: m = multiplet, b = broad, d = doublet, dd = doublet of doublets, t = triplet, s = singlet. Other abbreviations used: MeOH = methanol, EtOH = ethanol, EtOAc = ethylacetate, Et₂O = diethylether, TFA = trifluoroacetic acid, DIAD = diisopropylazodicarboxylate, Et₃N = triethylamine, BOP = Benzotriazole-1-yl-oxy-tris-(dimethylamino)-phosphonium hexafluorophosphate. DIPEA = diisopropylethylamine, DMAP = 4-(dimethylamino)pyridine, EDCI.HCl = 1-ethyl-3-(3'-dimethylaminopropyl)carbodiimide-HCl. Fast Atom Bombardment (FAB) mass spectrometry was carried out using a JEOL JMS SX/SX 102A four-sector mass spectrometer, coupled to a JEOL MS-MP9021D/UPD system program. Samples were loaded in a matrix solution (3-nitrobenzyl alcohol) on to a stainless steel probe and bombarded with Xenon atoms with energy of 3 KeV. During the high resolution FAB-MS measurements a resolving power of 10.000 (10% valley definition) was used.

3. Synthesis of rotaxanes **1** and **4** and the corresponding threads **3** and **5**



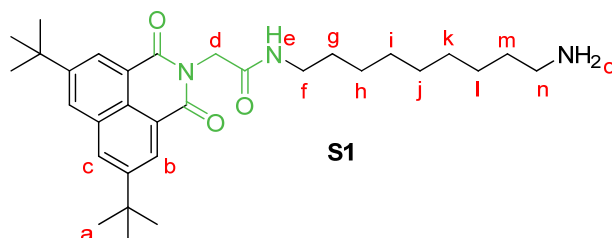


Scheme 1. (i) Glycine, Et_3N , EtOH, reflux, 2 h, 70 %; (ii) a) Pentafluorophenol, EDCI, HCl, DMAP, $0^\circ\text{C}\rightarrow\text{RT}$, CH_2Cl_2 , 4 h, 85 %; b) 1,9-diaminononane, CH_2Cl_2 , RT, 4 h, 78 %; (iii) *N*-(2,2-diphenylethyl)-succinic acid, Et_3N , CH_2Cl_2 , RT, 16 h; (iv) Isophthaloyl dichloride, *p*-xylylene diamine, Et_3N , CHCl_3 , RT, 20h, 30 %.

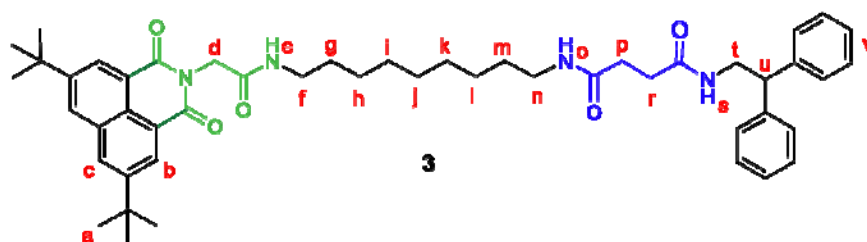


Scheme 2. (i) 1,12-diaminododecane, BOP, DIPEA, DMF, RT, 20h, 60 %; (ii) Isophthaloyl dichloride, *p*-xylylene diamine, Et_3N , CHCl_3 , RT, 20h, 8 %.

4. Details of synthesis and characterization

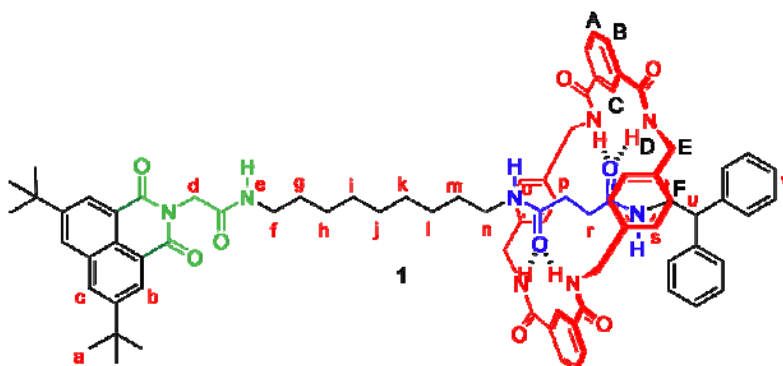


2-(Acetic acid)-5-8-di-*tert*-butyl-benzo[de]isoquinoline-1,3-dione (0.32 g, 0.87 mmol), DMAP (0.03 g, 0.26 mmol) and pentafluorophenol (0.19 g, 1.04 mmol) were dissolved in dichloromethane (30 mL) and cooled in an ice bath to 0°C. EDCI (1.04 mmol, 0.19 g) was added in small portions and reaction was continued overnight at room temperature. Solvents were removed and the residue was redissolved in dichloromethane (30 mL). 1,9-Diaminononane (0.83 mmol, 0.13 g) was added and the mixture was stirred for 16 h at room temperature. Reaction mixture was washed with HCl (1 M, 2 x 100 mL), brine (2 x 100 mL) and water (2 x 100 mL) before being dried by MgSO₄. Solvents were removed to give a white solid of **S1** (0.27 g, 78% over two steps). ¹H NMR (400 MHz, CD₃OD): δ = 8.68 (d, 2H, *J* = 2.0, H_b), 8.16 (d, 2H, *J* = 2.0, H_c), 5.77 (bs, 1H, H_e), 4.87 (s, 1H, H_d), 3.30 (td, *J* = 8.0, *J* = 4.0, 2H, H_f), 3.11 (t, *J* = 8.0, 2H, H_n), 1.51-1.46 (m, 22 H, H_a+H_g+H_m), 1.29-1.25 (m, 10H, H_h+H_i+H_j+H_k+H_l); ¹³C NMR (100 MHz, CDCl₃): δ = 166.9 (CO), 164.3 (CO), 150.1 (ArC), 131.9 (ArC), 129.5 (ArCH), 129.4 (ArCH), 124.8 (ArC), 121.5 (ArC), 43.0 (CH₂), 39.7 (CH₂), 35.1 (C_q), 31.0 (CH₃), 29.3 (CH₂), 29.1 (CH₂), 28.9 (CH₂), 26.7 (2xCH₂).

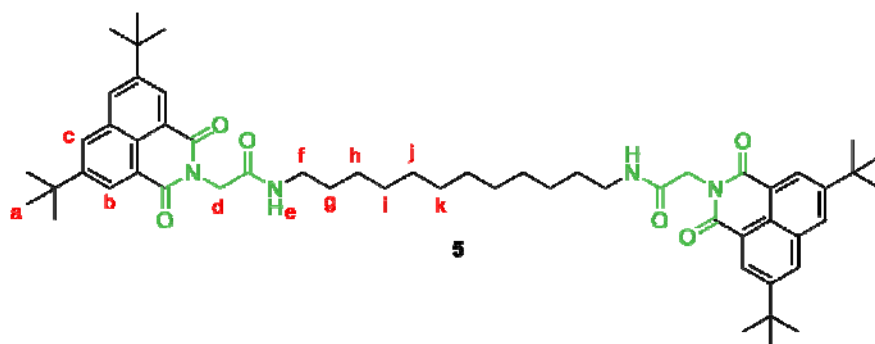


To a solution of amine **S1** (0.34 g, 0.67 mmol) and triethylamine (6.71 mmol, 941 μL) in dichloromethane (30 mL) under atmosphere of nitrogen (2,2-diphenylethyl)succinamic acid (0.74 mmol, 0.22 g) was added and the reaction was continued for 16 hours at room temperature. Additional portion of dichloromethane (50 mL) was added and the mixture was washed with HCl (1 M, 3 x 50 mL), saturated NaHCO₃ solution (3 x 50 mL), brine (1 x 50 mL), water (1 x 50 mL), dried over MgSO₄ and concentrated under reduced pressure. The resulting solid was purified by column chromatography on silica gel using a solvent gradient of CH₂Cl₂ to CH₂Cl₂ / MeOH (40:1) to obtain **3** as a white solid (0.21 g, 40%). ¹H NMR (400 MHz, CDCl₃): δ = 8.62 (d, *J* = 1.5, 2H, H_b), 8.12 (d, *J* = 1.5, 2H, H_c), 7.35 – 7.03

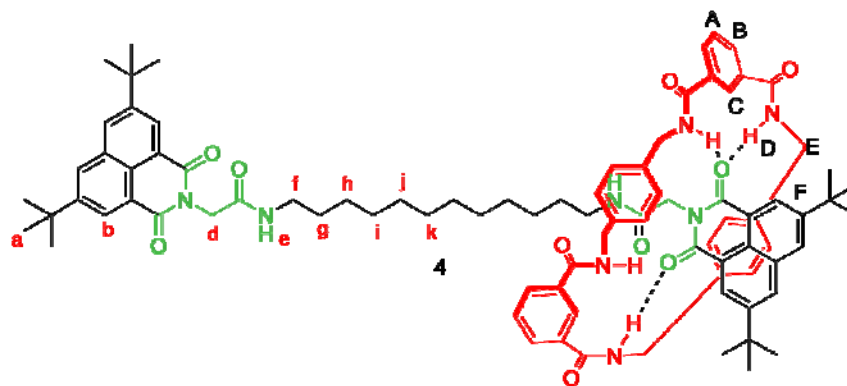
(m, 11H, H_v), 6.11 (bs, 1H, H_s), 5.99 (t, $J = 5.3$ Hz, 2H, H_o+H_e), 4.82 (s, 2H, H_d), 4.15 (t, $J = 8.0$, 1H, H_u), 3.84 (t, $J = 8.0$, 2H, H_t), 3.24 (dd, $J = 13.2$, $J = 6.6$, 2H, H_r), 3.12 (dd, $J = 13.0$, $J = 6.5$, 2H, H_n), 2.37 (s, 4H, H_p+H_r), 1.48-1.44 (m, 22H, H_a+H_g+H_m), 1.28-1.24 (m, 10H, H_h + H_i + H_j + H_k + H_l); ¹³C NMR (100 MHz, CDCl₃): $\delta = 172.2$ (CO), 171.9 (CO), 166.9 (CO), 164.3 (CO), 150.1 (ArC), 141.7 (ArC), 131.9 (ArC), 129.6 (ArCH), 129.5 (ArCH), 128.5 (ArCH), 127.9 (ArCH), 126.6 (ArCH), 124.9 (ArC), 121.5 (ArC), 50.4 (CH), 43.7 (CH₂), 42.9 (CH₂), 39.5 (CH₂), 39.4 (CH₂), 35.1 (C_q), 31.6(CH₂), 31.0 (CH₂), 29.3 (CH₂), 29.1 (CH₂), 28.9 (CH₂), 28.6 (CH₂), 26.4 (CH₂), 26.4 (CH₂), 23.5 (CH₂). HRMS (FAB, 3-NOBA matrix): $m/z = 787.5$ [M+H]⁺ (Calcd for C₄₉H₆₂N₄O₅ + H⁺: $m/z = 787.4$). Elemental analysis calcd for C₄₉H₆₂N₄O₅: C 74.78, H 7.94, N 7.12; found C 74.63, H 7.88, N 7.06.



The thread **3** (0.210 g, 0.266 mmol) and triethylamine (903 μ L, 6.34 mmol) were dissolved in chloroform (75 mL), and stirred vigorously whilst solutions of the *p*-xylylene diamine (0.43 g, 3.17 mmol) and isophthaloyl dichloride (0.64 g, 3.17 mmol) in CHCl₃ (20 mL) were simultaneously added over a period of 4 hours using a motor-driven syringe pump. The resulting suspension was stirred overnight and filtered through a pad of Celite to afford the crude product. The solvent was removed and the residue was subjected to column chromatography (silica gel, CH₂Cl₂: Acetone (9:1) to yield unreacted thread **3** (0.136 g, 65%) and rotaxane **1** (0.101 g, 30%) as white solids. ¹H-NMR (400 MHz, CD₃CN): $\delta = 8.57$ (d, $J = 1.8$, 2H, H_b), 8.45 (s, 2H, H_c), 8.28 (d, $J = 1.8$, 2H, H_e), 8.07 (dd, $J = 7.7$, $J = 1.4$, 4H, H_b), 7.79 (t, $J = 5.2$, 4H, H_D), 7.59 (t, $J = 7.8$, 2H, H_A), 7.36 – 7.18 (m, 10H, H_v), 7.14 (t, $J = 8.0$, 1H, H_e), 7.03 (s, 8H, H_F), 6.73 (t, $J = 4.0$, 1H, H_s), 6.65 (t, $J = 4.0$, 1H, H_o), 4.70 (s, 2H, H_d), 4.44 – 4.29 (m, 8H, H_{E+E'}), 4.11 (t, $J = 7.9$, 1H, H_u), 3.72 (dd, $J = 7.7$, $J = 5.8$, 2H, H_t), 3.02 – 2.86 (m, 4H, H_r+ H_n), 1.43 (s, 18H, H_a), 1.39 – 1.20 (m, 4H, H_g+ H_m), 1.15-1.11 (m, 10H, H_h+ H_i+ H_j+ H_k+ H_l), 1.04 (bs, 4H, H_p+ H_r); ¹³C NMR (100 MHz, CD₃CN): $\delta = 173.1$ (CO), 172.8 (CO), 167.1 (CO), 165.6 (CO), 164.1 (CO), 150.1 (ArC), 142.5 (ArC), 137.7 (ArC), 134.1 (ArC), 132.1 (ArC), 130.6 (ArCH), 129.5 (ArCH), 128.8 (ArCH), 128.4 (ArCH), 127.7 (ArCH), 126.5 (ArCH), 124.7 (ArC), 124.4 (ArCH), 121.8 (ArC), 50.2 (CH), 43.3 (CH₂), 43.1 (CH₂), 42.8 (CH₂), 34.7 (C_q), 30.2 (CH₃), 29.2 (CH₂), 29.1 (CH₂), 29.0 (CH₂), 28.8 (CH₂), 28.5 (CH₂), 28.4 (CH₂), 28.4 (CH₂), 28.3 (CH₂). HRMS (FAB, 3-NOBA matrix): $m/z = 1319.7$ [M+H]⁺ (Calcd for C₈₁H₉₀N₈O₉ + H⁺: $m/z = 1319.6$). Elem. Analysis calcd for C₈₁H₉₀N₈O₉: C 73.72, H 6.87, N 8.49; found C 73.62, H 6.75, N 8.63.



To a stirred solution of 2-(acetic acid)-5-8-di-*tert*-butyl-benzo[de]isoquinoline-1,3-dione (0.200 g, 0.544 mmol) in DMF (10 mL) under nitrogen BOP (0.318 g, 0.721 mmol) was added in one portion and the reaction mixture was stirred at room temperature for 0.5 h. Then DIPEA (6.63 μ L, 3.81 mmol) and 1,12-diaminododecane (0.052 g, 0.259 mmol) in DMF (5 mL) were added to the reaction mixture. After overnight stirring at room temperature DMF was removed under reduced pressure. The residue was purified by column chromatography on silica gel using CH_2Cl_2 / Acetone (94:6) as the eluent. Symmetrical thread **5** (0.349 g, 60%) was obtained as a white solid. ^1H NMR (400 MHz, CDCl_3): 8.68 (d, $J = 1.6$, 4H, H_b), 8.16 (d, $J = 1.6$, 4H, H_c), 5.79 (t, $J = 4.0$, 2H, H_e), 4.86 (s, 4H, H_d), 3.30 (td, $J = 8.9$, $J = 4.0$, 4H, H_f), 1.59-1.49 (m, 40H, $\text{H}_a + \text{H}_g$), 1.33-1.24 (m, 16H, $\text{H}_h + \text{H}_i + \text{H}_j + \text{H}_k$); ^{13}C NMR (100 MHz, CDCl_3): $\delta = 166.8$ (CO), 164.3 (CO), 150.1 (ArC), 131.9 (ArC), 129.6 (ArCH), 129.5 (ArCH), 124.9 (ArC), 121.5 (ArC), 43.0 (CH_2), 39.6 (CH_2), 35.1 (CH_2), 31.0 (CH_3), 29.2 (CH_2), 29.1 (CH_2), 28.9 (CH_2), 26.6 (CH_2). HRMS (FAB, 3-NOBA matrix): $m/z = 899.6$ $[\text{M}+\text{H}]^+$ (anal. Calcd for $\text{C}_{56}\text{H}_{74}\text{N}_4\text{O}_6 + \text{H}^+$: $m/z = 899.6$). Calcd for $\text{C}_{56}\text{H}_{74}\text{N}_4\text{O}_6$: C 74.80, H 8.29, N 6.23; found C 74.78, H 8.30, N 6.23.



Thread **5** (0.126 g, 0.140 mmol) was suspended in anhydrous CHCl_3 (100 mL) and triethylamine (472 μL , 3.36 mmol). Separate solutions of *p*-xylylene diamine (0.247 g, 1.82 mmol) and isophthaloyl dichloride (0.369 g, 1.82 mmol) in CHCl_3 (30 mL) were simultaneously added over a period of 5 hours at room temperature. After being stirred overnight, the suspension was filtered through a pad of Celite. The solvent was removed and the residue was subjected to column chromatography (silica gel, CH_2Cl_2 : Acetone (9:1) to yield unreacted thread (0.116 g, 92 %) and rotaxane (0.016 g, 8 %) as a white solid. ^1H NMR (500 MHz, CDCl_3) δ (ppm): 8.53 (s, 4H, H_b), 8.14 (bs, 10H, $\text{H}_c+\text{H}_B+\text{H}_C$), 7.94 (t, $J = 4.0$, 4H, H_D), 7.53 (t, $J = 8.0$, 2H, H_A), 7.04 (s, 8H, H_F), 6.52 (s, 2H, H_e), 4.43 (d, $J = 4.4$, $\text{H}_{E+E'}$), 4.27 (s, 4H, H_d), 2.89 (td, $J = 8.0$, H_f), 1.45 (s, 36H, H_a), 1.29-1.25 (m, 4H, H_g), 1.09 (bs, 16H, $\text{H}_h+\text{H}_i+\text{H}_j+\text{H}_k$); ^{13}C NMR (100 MHz, CDCl_3): $\delta = 166.6$ (CO), 164.9 (CO), 150.1 (ArC), 137.1 (ArC), 133.9 (ArC), 131.8 (ArC), 130.9 (ArCH), 129.6 (ArCH), 129.4 (ArCH), 128.9 (ArCH), 128.6 (ArCH), 124.8 (ArC), 121.4 (ArC), 44.6 (CH_2), 42.3 (CH_2), 39.6 (CH_2), 35.1 (CH_2), 31.0 (CH_3), 28.9 (CH_2), 28.7 (CH_2), 28.5 (CH_2), 26.4 (CH_2). HRMS (FAB, 3-NOBA matrix): $m/z = 1431.8$ [$\text{M}+\text{H}$] $^+$ (Calcd for $\text{C}_{88}\text{H}_{102}\text{N}_8\text{O}_{10} + \text{H}^+$: $m/z = 1431.8$). Elemental analysis calcd for $\text{C}_{88}\text{H}_{102}\text{N}_8\text{O}_{10}$: C 73.82, H 7.18, N 7.83; found C 73.71, H 7.22 N 7.79.

5. NMR spectra

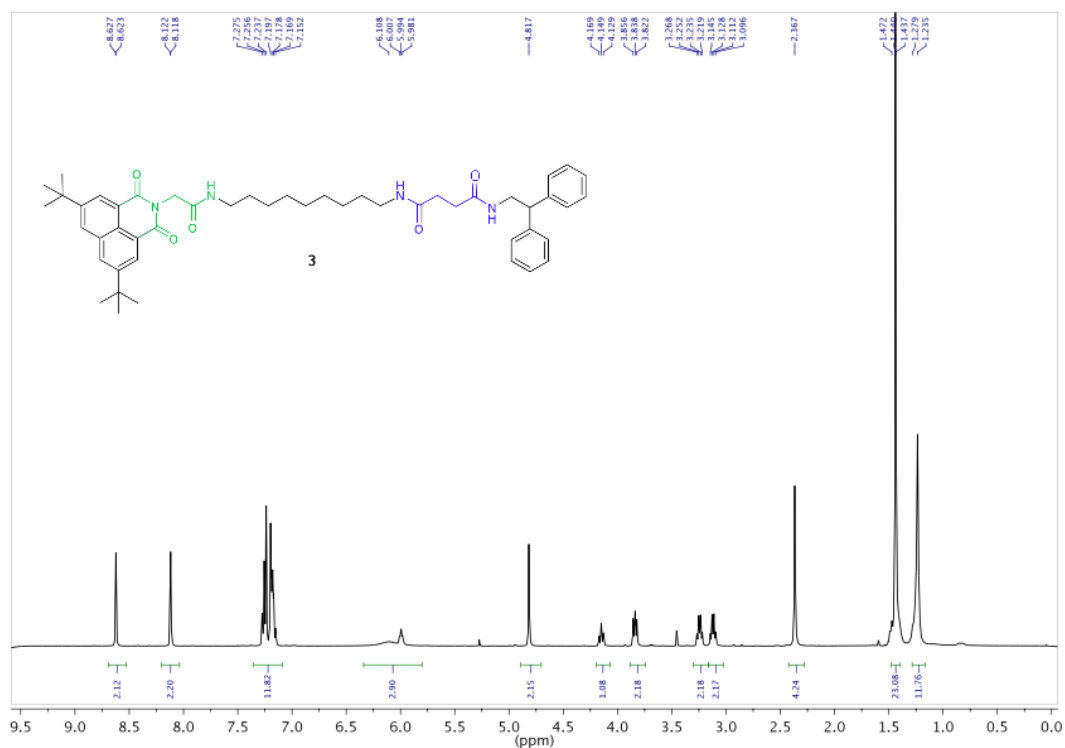


Figure S1. $^1\text{H-NMR}$ spectrum of compound 3 (400 MHz, CDCl_3 , 298 K).

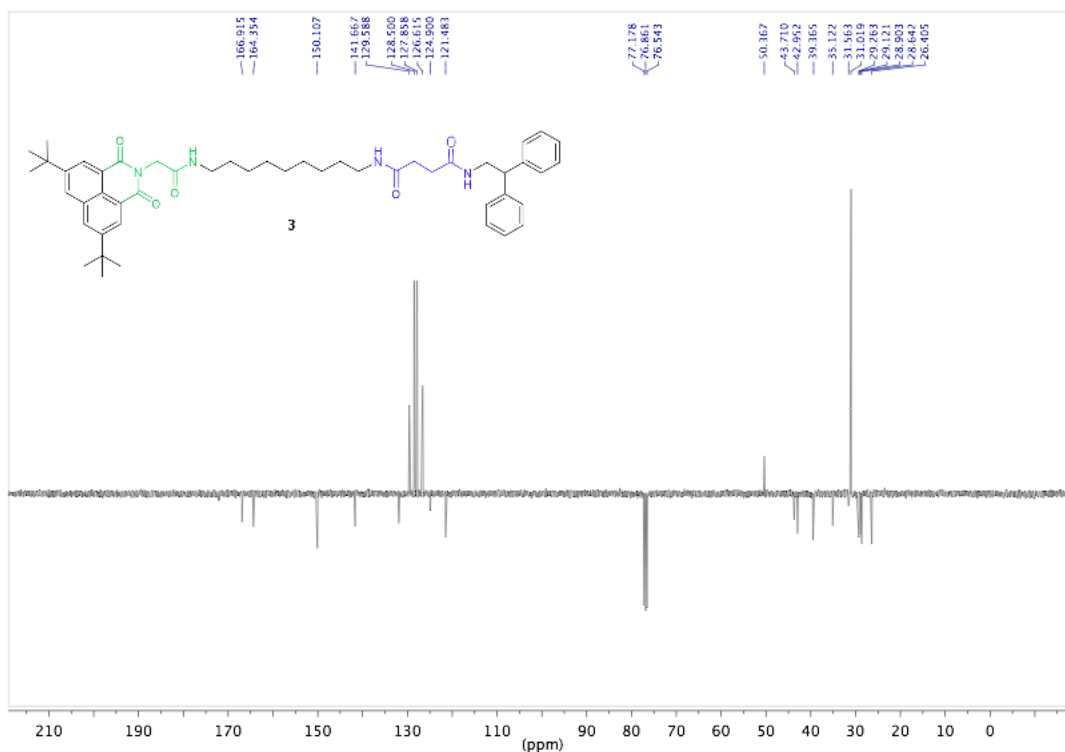


Figure S2. APT spectrum of compound 3 (400 MHz, CDCl_3 , 298 K).

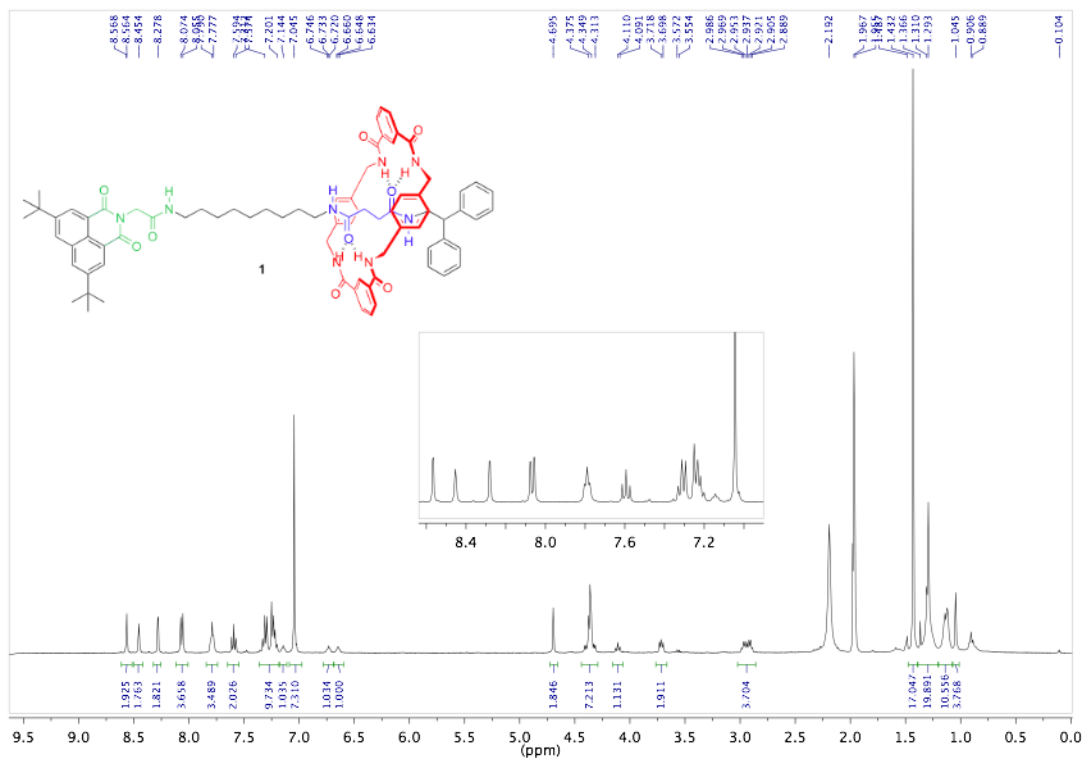


Figure S3. ¹H-NMR spectrum of compound 1 (400 MHz, CD₃CN, 298 K).

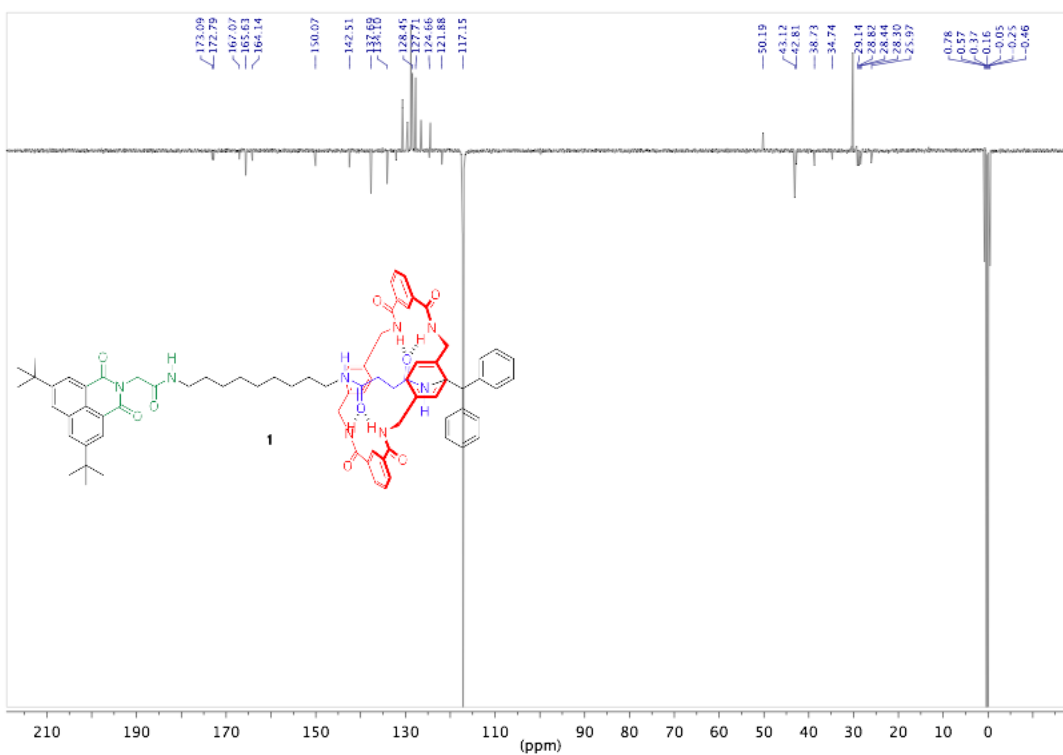


Figure S4. APT spectrum of compound 1 (400 MHz, CD₃CN, 298 K).

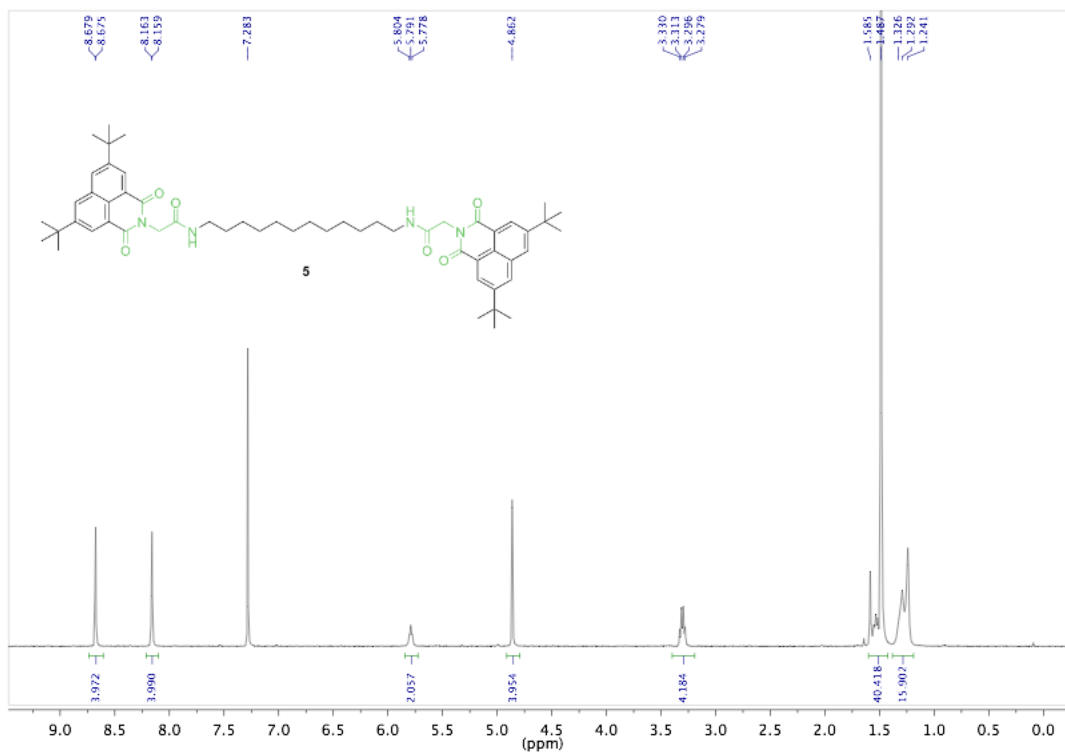


Figure S5. ¹H-NMR spectrum of compound 5 (400 MHz, CDCl₃, 298 K).

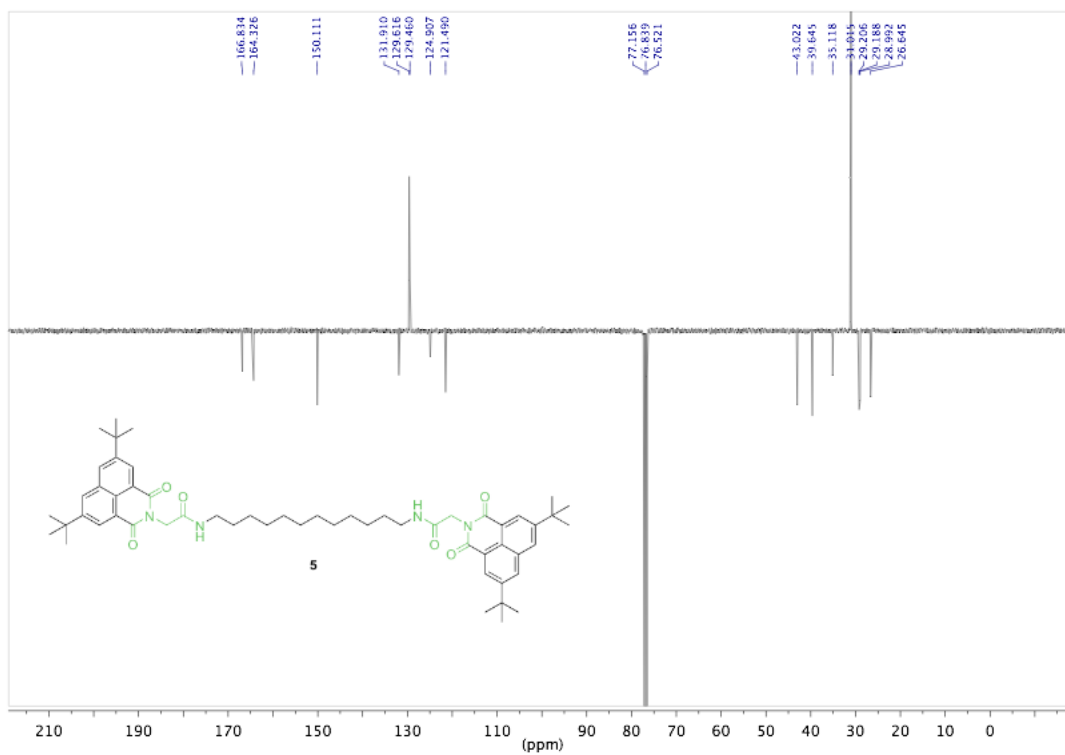


Figure S6. APT spectrum of compound 5 (400 MHz, CDCl₃, 298 K).

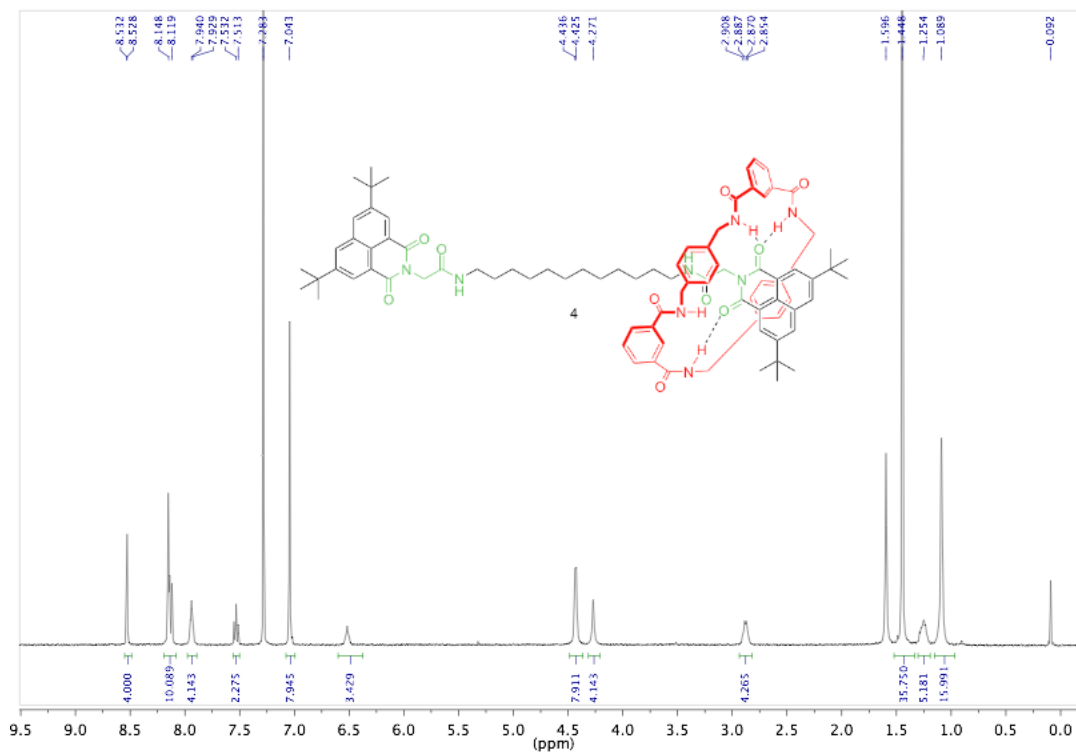


Figure S7. $^1\text{H-NMR}$ spectrum of compound 4 (500 MHz, CDCl_3 , 298 K).

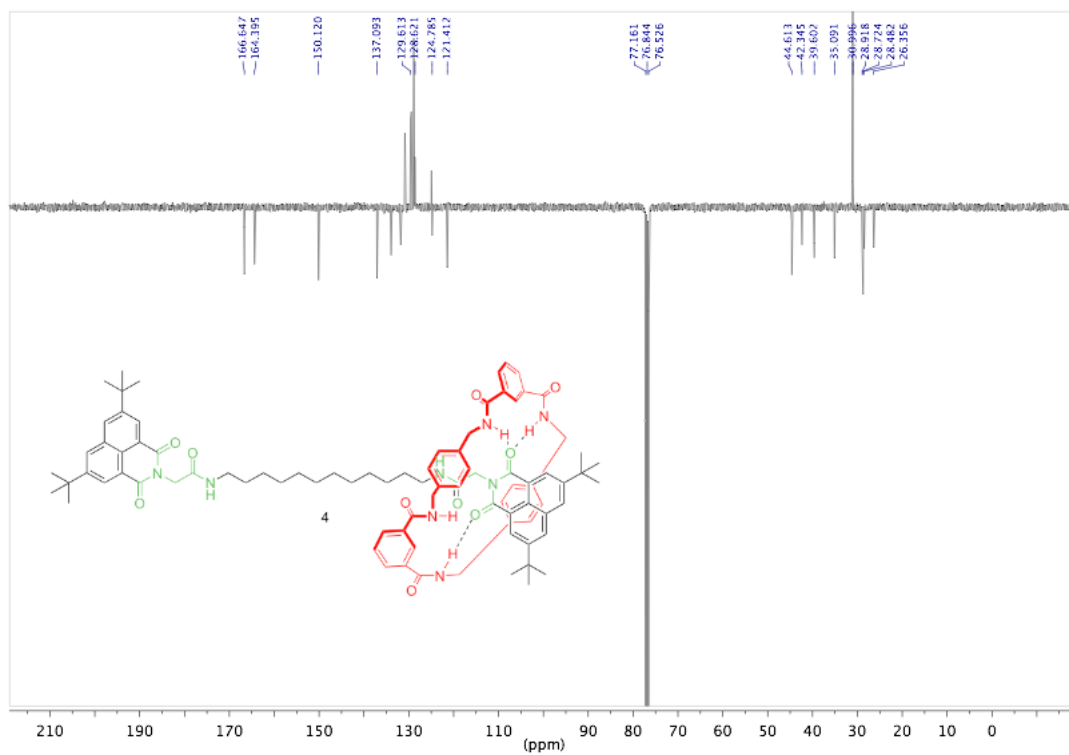


Figure S8. APT spectrum of compound 4 (400 MHz, CDCl_3 , 298 K).

6. Variable temperature $^1\text{H-NMR}$ spectra

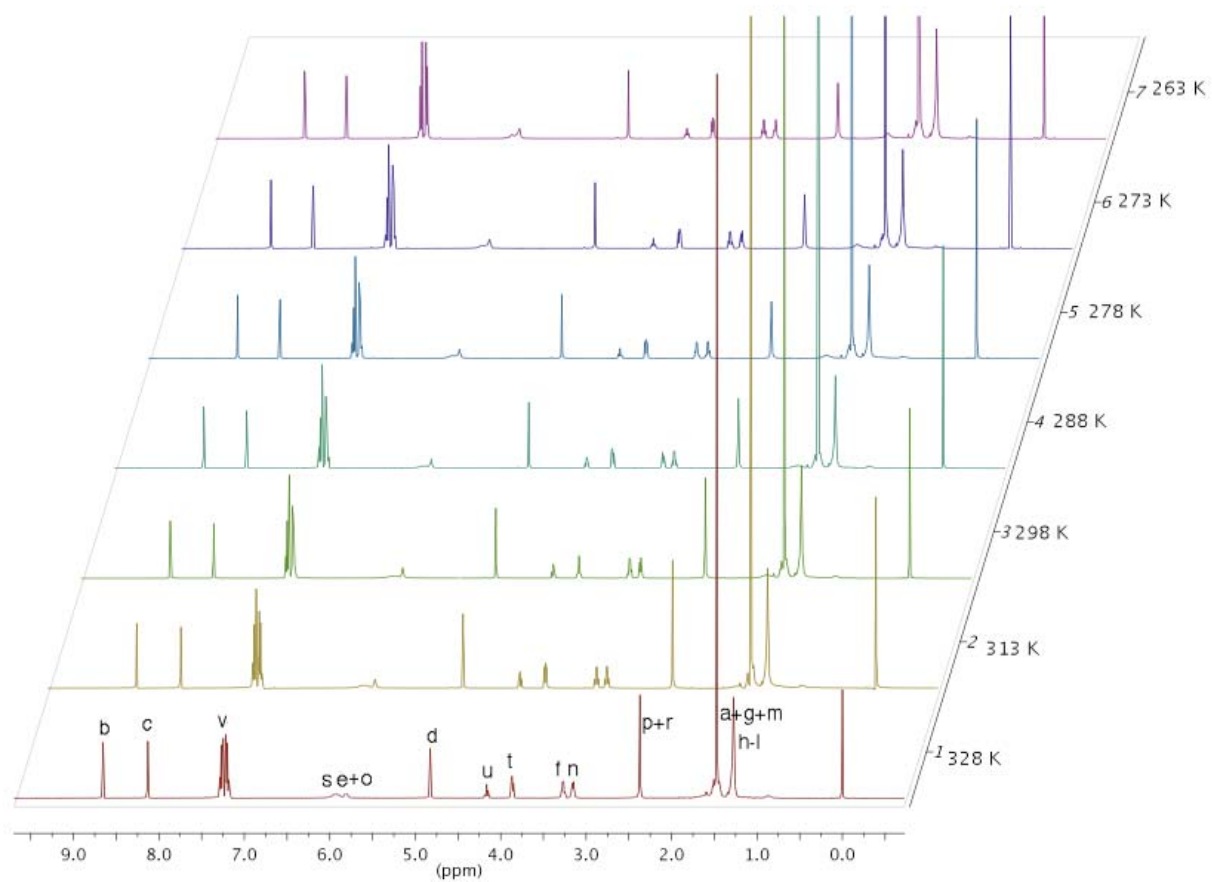


Figure S9. Temperature dependent $^1\text{H-NMR}$ spectrum of thread 3 (500 MHz, CDCl_3). The assignments correspond to the lettering shown in the experimental section.

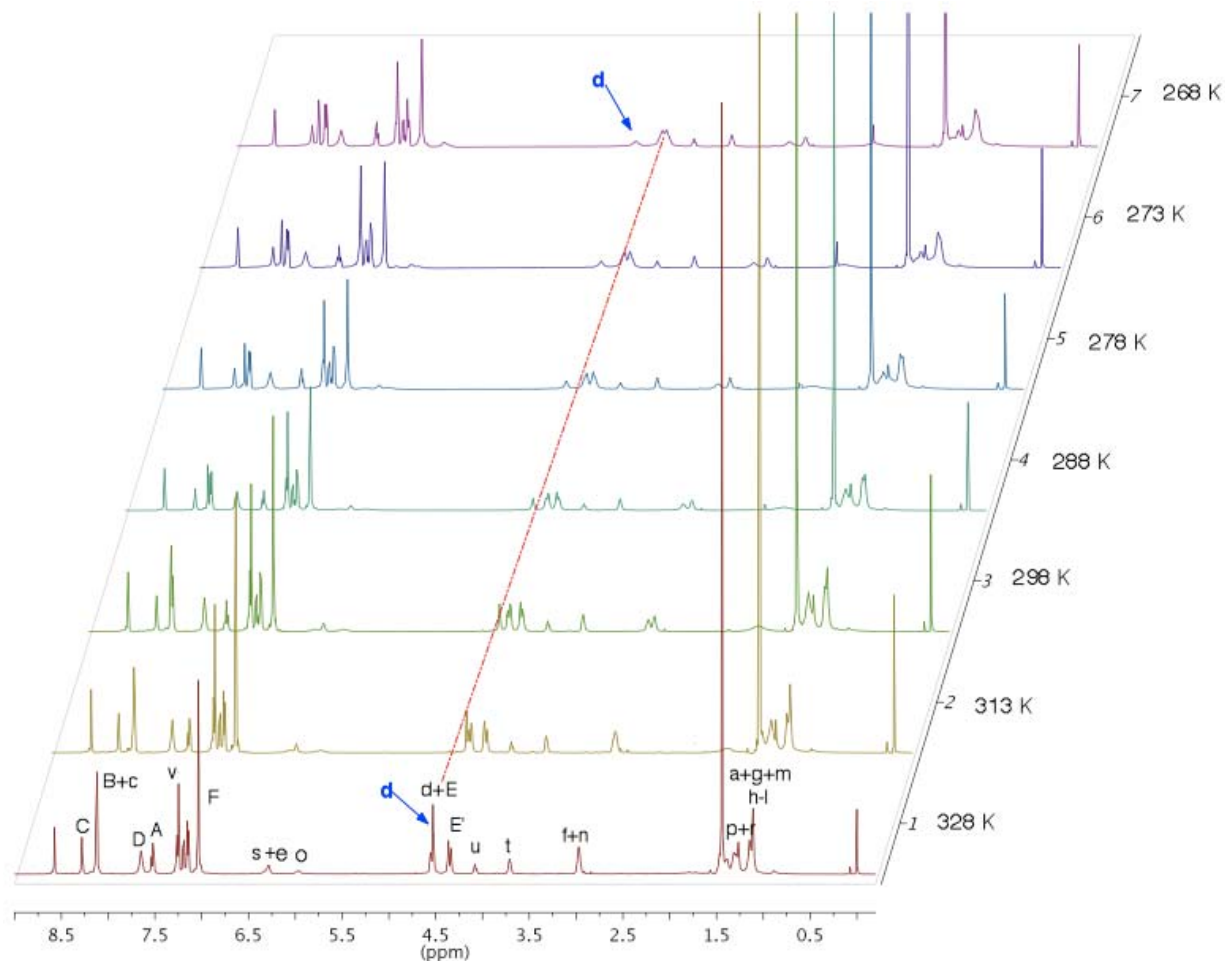


Figure S10. Temperature dependent ^1H -NMR spectrum of rotaxane **1** (500 MHz, CDCl_3). The assignments correspond to the lettering shown in the experimental section. Upon lowering the temperature resonances associated with H-d protons shift to higher frequency, indicating that the population of *ni*-co-conformer decreases with decreasing temperature.

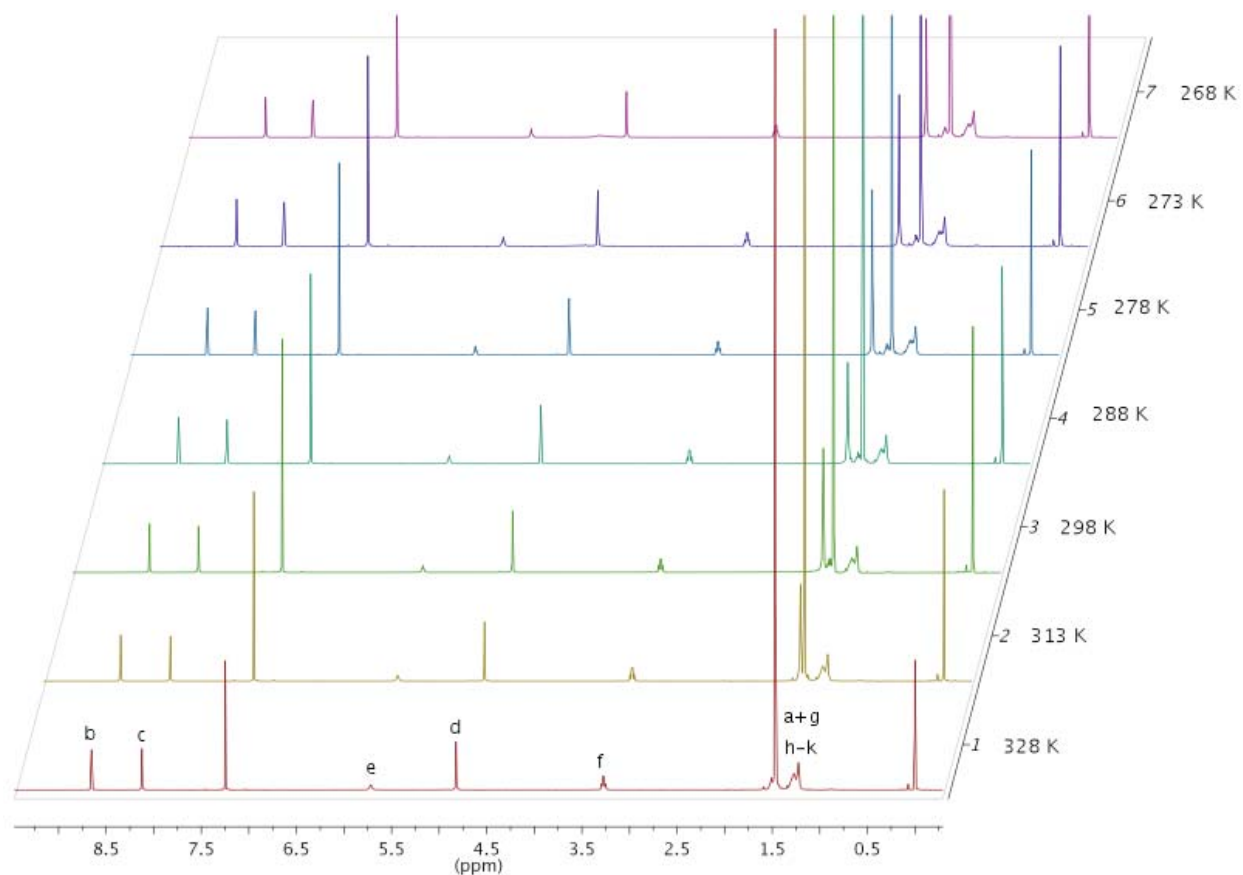


Figure S11. Temperature dependent ¹H-NMR spectrum of model thread **5** (500 MHz, CDCl₃). The assignments correspond to the lettering shown in the experimental section.

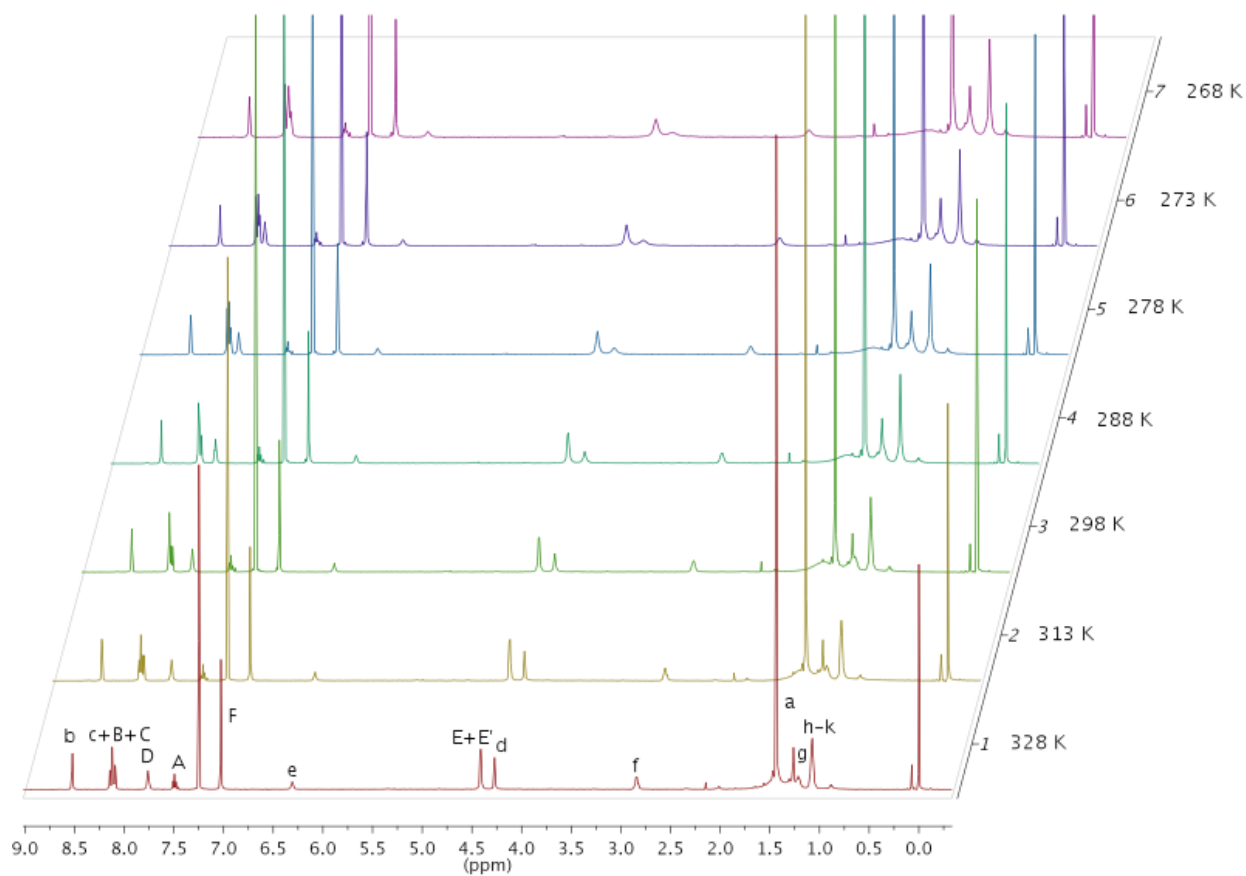


Figure S12. Temperature dependent ^1H -NMR spectrum of model rotaxane **4** (500 MHz, CDCl_3). The assignments correspond to the lettering shown in the experimental section.

7. Populations of translational isomers

The population of *ni* co-conformer (α_{ni}) was calculated according to equation 1. The δ 's in Table S1 refer to the chemical shifts of d protons in rotaxanes **1** and **3** and the corresponding threads **4** and **5**.

$$\alpha_{ni} = \frac{\delta_1 - \delta_2}{2(\delta_1 - \delta_2)} \quad (1)$$

Table S1. Chemical shifts (δ) of d protons in rotaxane **1**, rotaxane **3**, thread **4**, thread **5** and the population (α) of *ni* and *succ* co-conformers of **1**, temperature range 328-268 K.

Temp (K)	δ_1	δ_3	δ_4	δ_5	α_{ni}	α_{succ}
328	4.530	4.824	4.271	4.822	0.267	0.733
313	4.565	4.833	4.263	4.829	0.237	0.763
298	4.609	4.843	4.250	4.839	0.199	0.801
288	4.647	4.850	4.242	4.848	0.167	0.833
278	4.686	4.857	4.237	4.856	0.138	0.862
273	4.709	4.860	4.235	4.860	0.121	0.879
268	4.733	4.863	4.234	4.864	0.103	0.897

In figure S13 the fit according to eq. 2 is compared to a simple linear van 't Hoff plot, which clearly shows the inadequacy of the latter. The errors on $\ln K$ were calculated by propagation of the errors in the determination of the chemical shifts, which were estimated to be 0.003 ppm.

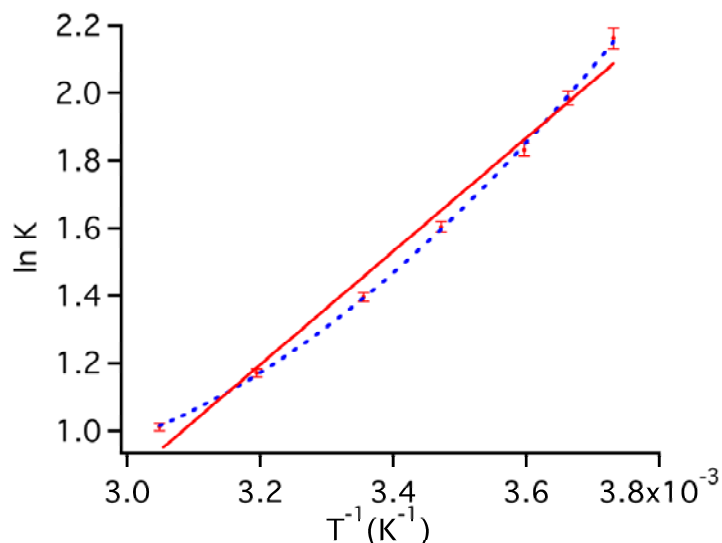


Figure S13. Fits to the data in Table S1. The non-linear curve (dashed line) is according to eq. 2 in main text. The error bars reflect the uncertainty in the estimation of $\ln K$. The solid line is the linear fit.

In the main text we interpreted the non-linear van 't Hoff plot using a model that allows a difference in the heat capacity of the *ni*- and *succ*-co-conformers. In addition we considered two possible experimental artifacts that could be alternative causes for the observed non-linearity of the van 't Hoff plot:

- (1) the use of the chemical shift values of the reference compound is an approximation; if the shape of the plot of the calculated $\ln K$ vs. T^{-1} would be very sensitive to the reference values, this may lead to an artificial curvature.
- (2) in addition to the two co-conformers for which we have clear evidence, there could be minor other co-conformers, in particular a bridged one.⁵

Numerical experiments showed that the precise values of the reference chemical shifts of a *ni*-CH₂-unit shielded by

the macrocycle are actually quite unimportant. Obviously, the fitted values of the thermodynamic parameters change somewhat when the reference values are changed, but as long as the reference shifts are reasonable, the plot remains distinctly curved.

A bridged co-conformer, in which the ring is hydrogen bonded to both amide stations, has been detected in other systems.⁵ In such a co-conformer shielding of the protons in the middle of the polymethylene chain is observed. In the present case, we see only a small shielding of the CH₂ groups of the polymethylene chain, very similar to the case of **2** (ref. 7 in main text). This is consistent with the argument given in the text that there cannot be more than about 5 % of this co-conformer.

In principle, the presence of the third co-conformer would induce an error in our analysis because we measure only the fraction of the *ni*-co-conformer, and assume that the rest of the population is the *succ*-co-conformer. If there is a third co-conformer, the actual fraction of the *succ*-form is smaller, and we slightly overestimate the free energy difference *ni-succ*. What is not a priori clear is whether this could induce a curvature in the van 't Hoff plot based on the apparent equilibrium ratios. Although this effect can probably be described analytically, we found it convenient to model it using simple spreadsheet calculations. We started from the enthalpy and entropy values obtained from our experimental data using the simple linear fit, as shown in Figure S13. This gives $\Delta H_1 = 3.1$ kcal/mol and $\Delta S_1 = 7.6$ cal mol⁻¹ K⁻¹. At 298 K this leads to a relative energy of $\Delta G_1 = 0.86$ kcal/mol for the *ni* form. A plot of ln K vs. T⁻¹ obviously gives a linear relation.

If the third co-conformer amounts to 5% ($\alpha_3 = 0.05$), its relative free energy $\Delta G_2 = \Delta H_2 - T\Delta S_2$ at room temperature with respect to the *succ* co-conformer is +1.6 kcal/mol. The latter value can be obtained using different combinations of ΔS_2 and ΔH_2 ; ΔH_2 can be entered in the spreadsheet and ΔS_2 is adapted to yield the required free energy difference to give 5 % of the third co-conformer at 298 K. In figure S14 we show some sets of approximate ln *K* values that are calculated neglecting the third co-conformer (i.e. assuming $K = \alpha_{ni} / (1 - \alpha_{ni})$), compared with the correct one (i.e. $K = \alpha_{ni} / (1 - \alpha_{ni} - \alpha_3)$, in blue). Using reasonable values of the parameters (-4 kcal/mol $< \Delta H_2 < 4$ kcal/mol) the slopes and intercepts of the fits change by < 10%. These are the black and red symbols in Figure S14. Detectable curvature of the plot arises only if one allows a much higher population of the third co-conformer, and an opposite sign of the relative entropies for the *ni*-co-conformer and the third co-conformer. Still, even with 15% of the third co-conformer (green symbols in Figure S14) – which is much more than the < 5 % indicated by our NMR data– the curvature of the van 't Hoff plot is much smaller than what we derived in our analysis. Thus, the curvature is not an artifact due to the inaccuracy of our model.

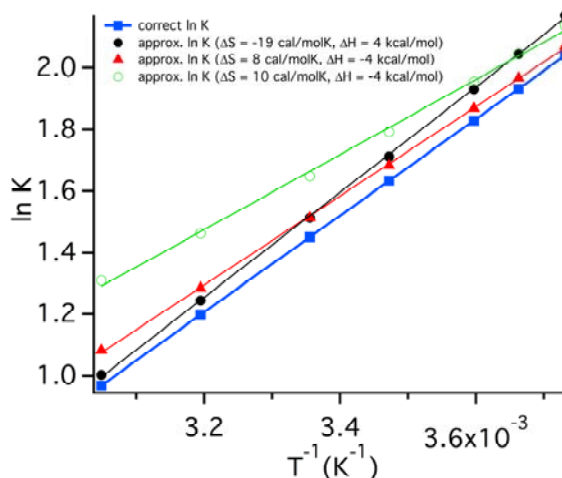


Figure S14. Model calculations of van 't Hoff plots in which heat capacity differences are not included. The blue squares represent the correct linear relation for $\ln(\alpha_{ni} / \alpha_{succ})$; the black filled circles and the red triangles are calculated for $\alpha_3 = 0.05$ at 298 K with different values of ΔS_2 and ΔH_2 . The lines are linear fits. The open green circles represent a case of for $\alpha_3 = 0.15$ at 298 K. This shows a slight curvature, but such a population of the third conformer is in conflict with our NMR data.

8. References

- 1 A. Altieri, G. Bottati, D. A. Leigh, J. K. Wong and F. Zerbetto, *Angew. Chem. Int. Ed.*, 2003, **42**, 2296-2300.
- 2 A. Altieri, F. G. Gatti, E. R. Kay, D. A. Leigh, D. Martel, F. Paplucci, A. M. Z. Slawin and J. K. Y. Wong, *J. Am. Chem. Soc.*, 2003, **125**, 8644-8654.
- 3 H. Li, X. Wang and C. Zheng, *Synt. Commun.*, 2006, **36**, 1933-1940.
- 4 M. D. Best, A. Brik, E. Chapman, L. V. Lee, W. C. Cheng and C. H. Wong, *ChemBioChem*, 2004, **5**, 811-819.
- 5 A. Altieri, G. Bottari, F. Dehez, D. A. Leigh, J. K. Y. Wong and F. Zerbetto, *Angew. Chem. Int. Ed.*, 2003, **42**, 2296-2300.